

The application of BEM in the Membrane structures interaction with simplified wind

Xu Wen[†], Ye Jihong[‡] and Shan Jian^{††}

School of Civil Engineering, Southeast University, Si Pai Lou 2#, Nanjing 210096, China

(Received October 31, 2007, Accepted January 14, 2009)

Abstract. Membrane structures are quite sensitive to wind and therefore the fluid-solid interaction can not be neglected in dynamic analysis. A boundary element method (BEM) for 3D simulation of wind-structure interaction in tensile membrane structures is presented in this paper. The flow is treated as incompressible and potential. The flow field is solved with boundary element method codes and structural simulation is performed by finite element method software ANSYS. The nonlinear equations system is solved iteratively, with segregated treatment of the fluid and structure equations. Furthermore this method has been demonstrated to be effective by typical examples. Besides, the influence of several parameters on the wind-structure interaction, such as rise-span ratio, prestress and the wind velocity are investigated according to this method. The results provide experience in wind resistant researches and engineering.

Keywords: membrane structures; fluid-structure interaction; boundary element method.

1. Introduction

In recent years, the tensile surface structure business has grown considerably, and is predicted to grow further. Such structures are becoming bigger and more sophisticated. More clients are interested in using them but they are still considered to be special – a new technology (Forster and Mollaert 2004). These structures have the advantages of nice aesthetic shape, fast installation, the reduction of construction cost, superior earthquake-resistant and fire-resistant performance. However, membrane structures are sensitive to wind. Consequently wind load plays an important role in these structures design. Many researches have been carried out about it; nevertheless, Computational Wind Engineering is in its infancy and has a long way to go to become truly useful to the design practitioner (Theodore 1997). The lack of knowledge about possible fluid-structure interaction effects led to collapse in the past, e.g., though characteristics of natural wind and wind pressures on design of buildings against severe wind were considered in the project of Jeju World Cup Stadium, which was built in Jeju Island, Korea. The roof claddings of this building were still torn and lifted off during the typhoon “Rusa” and “Fengshen”.

Different from conventional structures, tensile membrane structures are the flexible systems and their stiffness is provided by geometrical cured surface and prestress. Wind induces large

[†] Ph.D., Corresponding author, E-mail: slowlysmell@yahoo.com.cn

[‡] Professor, E-mail: yejihong@seu.edu.cn

^{††} Professor, E-mail: shanjian@hotmail.com

deformation and strong vibration of these flexible structures. Here, large deflection or vibration of the membrane surface has affected on the wind pressure distributions on structural surface. This procedure is called “wind-structure interaction” or “aero-elasticity”. Wind effects can define decisive design loads and therefore require in-depth analysis. The development of the methods for fluid-structure interaction is a topic of wind engineering researches. Analyses are usually carried out through wind tunnel tests, analytical methods, and numerical algorithms.

At presents, wind tunnel experiments are generally applied to determine wind loads of complex buildings in wind engineering. The majority of wind tunnel tests are carried out on rigid models that do not take into account changes in the applied pressure distribution due to deflection of the membrane surface. Hence rigid model tests are not the most suitable type for deflection-sensitive membrane surfaces. A more complex aeroelastic wind tunnel test to investigate dynamic effects, such as galloping and flutter, could be more suitable for such a structure. This would incorporate in the model a surface that deflects in a similar way to the full size structure. However, these models are very complex to build and do not always provide very consistent answers (Forster and Mollaert 2004, Irwin and Wardlaw 1979, Uematsu and Uchiyama 1986). Therefore, the valuable aeroelastic models are seldom in this field. Until recently, there is some lack of an agreement about the structural vibration modes and the reasons for structural aeroelastic instability. In other words, there are few appropriate rules, which can be applied in practice directly.

In simplified aeroelastic model method, some necessary hypothetical conditions are induced to modify the models. It means that additional aerodynamic feedback terms, such as added mass, aerodynamic damping and aerodynamic stiffness, are added to the wind load on the static structural surface to simulate the process of wind-structure interaction. Thus in time domain, we can obtain structural responds under wind loads by solving motion equations, which based on nonlinear finite element method. Here, aerodynamic stiffness is taken into account only in pneumatic structures. So in tensile membrane structures, it can be omitted. Added mass can be computed through thin aerofoil theory. Examples are to be found in Minami 1998, Yadykin and Teneto and Levin 2003. Aerodynamic damping is very difficult to determine in analysis. Some researchers (e.g., Irwin and Wardlaw 1979, Sun *et al.* 2003 and Pospisil *et al.* 2006) treat aerodynamic damping as acoustic damping. However, these simplified areoelastic model methods lack of experimental validation. Furthermore, the internal mechanism of dynamic destabilization can not be explained clearly though previous theories yet. Zhang, Wu and Shen 2002 suggest that added aerodynamic items also could be obtained by wind tunnel tests.

Computational fluid dynamic simulation method is increasing application with the development of computer technology. Such a numerical simulation is very challenging in the cases of interaction between structure and wind. Generally, two different types of approaches for the numerical simulation exist: monolithic and partitioned strategies (e.g., Wüchner Kupzok and Bletzinger 2007). In a so-called monolithic approach, governing equations of coupled fields are formulated in each time step, including fluid governing equation and structure governing equation. All physical fields are solved in one single numerical model. In a partitioned fluid-structure interaction simulation, the fluid and the structure simulation work are together in a staged algorithm. They exchange deformations and stresses at respective boundaries that are on a common interface. Here, the interface is the surface of structure wetted by fluid, and the exchange on which has to meet requirements of the kinematic and dynamic continuity. The monolithic approach is usually applied in theoretic analysis of coupled fields. Due to the difference of grids requirements in liquid field and structure field, the grids of the two fields are not match, which leads to the being restricted within

limits. The main advantage of the partitioned approach is the fact that specialized and well-tested simulation codes for each physical field can be brought together to solve the coupled problem. Moreover, this approach occupies less memory. Therefore, partitioned approach is widely used in simulation of fluid-structure interaction.

Hübner, Walborn and Dinkler 2002 present monolithic approach for time-dependent fluid-structure coupling. Coincident time and space finite element method was applied in discretizing and solving simultaneous equations, including incompressible flow Navier-Stokes equation, motion equation, energy conservation, geometric continuity at coupling interface. In conclusion, separation eddy and structural response were described in the results. However, the examples in that paper were restricted to two-dimensional problems. A set of partitioned coupling approaches (Glück *et al.* 2001, 2003, Giovanni 2002) for time-dependent fluid-structure interactions were applied to membrane structures with large displacements. In the flow field, standard k - ϵ and k - ω models were induced and a three-dimensional, finite volume method was used to solve incompressible Navier-Stokes equations. The finite element program performs the structural simulations. Examples showed the structural response delayed quickly under turbulent flow conditions at a high wind speed leading to a steady deformation state. But the validity of this numerical method remained to confirm in contrast with actual observation data. Sygulski 1997 proposes a numerical method of analysis membrane stability in which the flow is treated as incompressible and potential. The velocity potential of the air satisfied the Laplace equation, the solution of which was described expressed as a boundary integral equation. The boundary conditions on the surface are the Neumann type. Finite element method and boundary element method were used to solve the equations that were described by differential and integral equations respectively. Dimensionless stability analyses of circular, square and rectangular membranes were presented.

Current CFD software has no appropriate function in simulation of fluid-structure interaction, especially to the complicated 3D problems, e.g., wind-membrane structures. Moreover, amount of calculation is prodigious to these problems. Shen and Wu 2006 present a simplified numerical approach of time-dependent wind-structure interaction. The general idea of the approach was to divide the structural response into three components: mean response, background response and resonant response. Mean response and background response were regarded as static interaction. The last component was a transient interaction process. Due to different characteristics of each component, different methods were adopted respectively. For static interaction, CFD simulation was used. For transient interaction, nonlinear random vibration analysis in time domain was adopted, considering the influence of added mass and aerodynamic damping. Even if in this simplified method, simulation the wind-structure interaction by using CFD software will still consume a great deal of computer time and resource. The reason is that it costs superabundant time and it is easy to make mistakes in the process of meshing for complex structures. Generally speaking, the proceeding of meshing takes longer time than actually computing in CFD software simulation. At present, it is about 80 percent of time in meshing grids, and is about 20 percent of time in computing. Membrane structures often produce large deformation and big vibration under wind load, so the grids in flow field have to be meshed afresh. Therefore, this method can not essentially resolve the problem of excessive computing time and resource.

An approach based on boundary element method is presented in this paper to simulate wind-structure interaction. Here a partitioned solution scheme is chosen. Essential hypotheses are introduced, i.e., the flow is treated as incompressible and potential. Boundary element method program is adopted in flow field, while the structural simulations are performed by ANSYS, finite

element software considering the geometrical non-linear problem. From the beginning, the wind pressure distribution on the structural surface of original form is obtained by employing boundary element method codes. Subsequently, structural deformation under this wind pressure can be gained by using ANSYS software. Then, boundary element method program will be adopted again to simulate the wind pressure distribution on deformed surface. The following step is to calculate structural deformation under the wind pressure that is just gotten in precedent step by ANSYS software. The iterative procedure is as mentioned above. When the displacements of the iteration circle approximate to those of previous iteration, the iterative process ends. The structural deformations and wind pressure distribution at this moment are in steady state. If the displacements between two iteration are not same, the procedure will not ended until the solution is satisfied the convergence criteria. In meshing process, boundary element method, which grids are merely meshed on the boundaries, differs from finite element method. For transforming the problem to boundary, the dimension of this problem reduces, so it will save a great deal of memory capacity and computing time. Hence, boundary element method has the superiority in flow field solving. However, boundary element method is seldom applied in wind-structure interaction. Corresponding Sygulski 1997, which is mentioned in previous parts, presented a numerical method based on boundary element method. But This method avoids solving complex nonlinear differential equation, and distinguishes stability of the membrane motion through the analysis of linearized nonlinear system equation eigenvalue. Therefore it is only restricted in the membrane structure stability analysis.

2. Fluid field hypothesis

The air is treated as incompressible and inviscid. It is assumed that the flow is potential and three-dimensional and ignored turbulence at the same time in this study. The hypotheses above simplify the motion equations. Thus, we can utilize the existing mathematical tools to simulate the flow around structures. The membrane is pre-stressed and enclosed construction. So the air only flows over the membrane outside surface. The model of fluid field around the membrane is similar to a wind tunnel (see Fig. 1). The structure locates in around the 1/3 front of the bottom. The boundary conditions of top surface, front side surface and back side surface of this flow field are velocity types, which normal velocities are all zeros. The procedure of fluid-structure interaction is considered a steady state and static in this research, so it is time-independent. Therefore, the normal velocities of the flow field bottom and the membrane surface are also zeros. The boundary condition of left side surface and right side surface are also the type of velocity. The left side surface is entrance boundary and the right side surface is outlet boundary, supposing which both have sufficient distance to the structure. The normal velocity of left side is $-V_\infty$. V_∞ is the remote

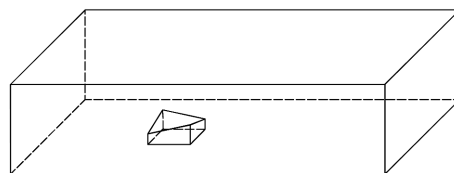


Fig. 1 Flow field

air flow velocity and the negative sign means that the outward normal direction to this surface is opposite to the inflow direction. The normal velocity of right side is V_∞ .

3. Computation of wind pressure distribution on membrane structures

The flow around the membrane structure is assumed potential flow. Potential flow, namely, irrotational flow, is applied in many domains while the viscosity of water or air can be omitted.

The relation of potential to velocity is as following

$$\mathbf{u} = \nabla\phi(x, y, z, t) \text{ or } u_i = \frac{\partial\phi}{\partial x_i} \tag{1}$$

where ϕ is the potential function and \mathbf{u} is the air flow velocity vector.

The potential equation of motion can be written

$$\frac{\partial u_i}{\partial t} + u_j \frac{\partial u_i}{\partial x_j} + \frac{1}{\rho} \frac{\partial p}{\partial x_i} + \frac{\partial F}{\partial x_i} = \frac{\partial}{\partial x_i} \left(\frac{\partial\phi}{\partial t} + \frac{1}{2} \frac{\partial\phi}{\partial x_j} \frac{\partial\phi}{\partial x_j} + P + F \right) = 0 \tag{2}$$

Here ρ , p , F and P are the density of air flow, static pressure, body force and pressure force. Integrating Eq. (2) gives

$$\frac{\partial\phi}{\partial t} + \frac{1}{2} \frac{\partial\phi}{\partial x_j} \frac{\partial\phi}{\partial x_j} + P + F = f(t) \tag{3}$$

This is the famous Bernoulli equation. In the case of potential problems, the motion equation is converted into Bernoulli equation. The velocity potential of the air satisfied the Laplace equation. Therefore, we may solve Bernoulli equation instead of the motion equations in practice.

The continuity equation of steady incompressible ideal fluid is

$$\nabla \cdot \mathbf{u} = 0 \tag{4}$$

Substituting now the Eq. (1) into Eq. (4) gives

$$\nabla \cdot \nabla\phi = \nabla^2\phi = \frac{\partial^2\phi}{\partial x_i \partial x_i} = 0 \tag{5}$$

Eq. (5) is Laplace equation. The flow around the membrane is potential and the velocity potential of the air flow satisfies Laplace equation. The potential solution of a Laplace equation can be obtained according to the determining solution conditions. Furthermore, pressure can be calculated by Bernoulli equation.

The determining solution problem of Laplace equation is

$$\begin{cases} \nabla^2\phi = 0 \text{ in } \Omega \\ \phi = \bar{\phi} \text{ on } \Gamma_1 \quad (\text{Essential Condition}) \\ q = \frac{\partial\phi}{\partial n} = \bar{q} \text{ on } \Gamma_2 \quad (\text{Natural Condition}) \end{cases}$$

where Ω represents two or three dimensional domain, in which is the solution of a Laplace

equation. Γ is the boundary and n is the normal to the boundary. In this paper, the boundary conditions are velocity conditions, i.e., natural conditions and therefore the equation above can be rewritten

$$\begin{cases} \nabla^2 \phi = 0 & \text{in } \Omega \\ q = \frac{\partial \phi}{\partial n} = \bar{q} & \text{on } \Gamma \end{cases} \quad (6)$$

The weighted residual formulation of Eq. (6) can be written as

$$\int_{\Omega} (\nabla^2 \phi) w d\Omega = \int_{\Gamma} (q - \bar{q}) w d\Gamma \quad (7)$$

where w is a weighted function.

By using integration by parts and Green formula, one can transform the term of the left-hand side of Eq. (7) into the following expression

$$\int_{\Omega} (\nabla^2 \phi) w d\Omega = \int_{\Gamma} w \left(\frac{\partial \phi}{\partial n} \right) d\Gamma - \int_{\Gamma} \phi \left(\frac{\partial w}{\partial n} \right) d\Gamma + \int_{\Omega} \phi \nabla^2 w d\Omega \quad (8)$$

Using notations

$$q = \frac{\partial \phi}{\partial n}$$

$$p = \frac{\partial w}{\partial n}$$

we could express the integral equation as

$$\int_{\Omega} (\nabla^2 \phi) w d\Omega = \int_{\Gamma} w q d\Gamma - \int_{\Gamma} \phi p d\Gamma + \int_{\Omega} \phi (\nabla^2 w) d\Omega \quad (9)$$

Substituting Eq. (9) into Eq. (7) then combining Eq. (6), one obtains

$$- \int_{\Omega} (\nabla^2 w) \phi d\Omega + \int_{\Gamma} p \phi d\Gamma = \int_{\Gamma} w q d\Gamma \quad (10)$$

This is an important equation as it is the starting point for the application of the boundary element method. Notice that the integral domain of the first term on the left side of Eq. (10) is in Ω and the integrand is $(\nabla^2 w) \phi$. The aim is now to render Eq. (10) into a boundary integral equation. It is done by using a special type of weighting function called the fundamental solution.

Let w be fundamental solution for the following equation

$$\nabla^2 w + \delta(\mathbf{X} - \mathbf{X}_i) = 0 \quad (11)$$

$$\text{where } \delta(\mathbf{X} - \mathbf{X}_i) = \begin{cases} \delta(x - x_i, y - y_i) & \text{for 2D} \\ \delta(x - x_i, y - y_i, z - z_i) & \text{for 3D} \end{cases}$$

where $\delta(\mathbf{X} - \mathbf{X}_i)$ represents a Dirac function (see appendix), which tends to infinity at point $\mathbf{X} = \mathbf{X}_i$ and is equal to zero anywhere else.

Introducing $\nabla^2 w = -\delta(\mathbf{X} - \mathbf{X}_i)$ into Eq. (10), one can obtain

$$\int_{\Omega} \delta(\mathbf{X} - \mathbf{X}_i) \phi d\Omega + \int_{\Gamma} p\phi d\Gamma = \int_{\Gamma} wq d\Gamma$$

The integral of a Dirac delta function multiplied by any other function is equal to the value of the latter at the point \mathbf{X}_i . Hence

$$\int_{\Omega} \delta(\mathbf{X} - \mathbf{X}_i) \phi d\Omega = \phi(\mathbf{X}_i) = \phi(x_i, y_i, z_i) = \phi^i$$

Eq. (10) now can be rewritten as

$$\phi^i + \int_{\Gamma} p\phi d\Gamma = \int_{\Gamma} wq d\Gamma \tag{12}$$

For a three dimensional domain the fundamental solution of Eq. (11) is

$$w(x, y, z; x_0, y_0, z_0) = \frac{1}{4\pi r}$$

where $r = \sqrt{(x-x_i)^2 + (y-y_i)^2 + (z-z_i)^2}$.

And for a two dimensional domain, the fundamental solution of Eq. (11) is

$$w(x, y; x_0, y_0) = \frac{1}{2\pi} \ln \frac{1}{r}$$

where $r = \sqrt{(x-x_i)^2 + (y-y_i)^2}$.

Eq. (12) is valid for any point within Ω domain. When the point \mathbf{X}_i is on Γ , i.e., \mathbf{X}_i is a boundary point, the Eq. (12) can be written as the following expression. The deduced procedure is omitted. See also references Brebbia and Dominguez 1992 and Gao and Davies 2002.

$$\frac{1}{2} \phi^i + \int_{\Gamma} p\phi d\Gamma = \int_{\Gamma} wq d\Gamma \tag{13}$$

The boundary integral Eq. (13) is for smooth boundary points. When the boundary points locate at a corner, the boundary equation is

$$c^i \phi^i + \int_{\Gamma} p\phi d\Gamma = \int_{\Gamma} wq d\Gamma \tag{14}$$

where $c^i = \begin{cases} \frac{\alpha}{2\pi} & \text{for 2D problem} \\ \frac{\alpha}{4\pi} & \text{for 3D problem} \end{cases}$ and α is the internal angle of the corner in radians.

The next step is to generate the equation system by boundary integral equation discretization. Firstly, the boundary is divided into n segments or elements, as follows

$$\Gamma = \sum_{j=1}^n \Gamma_j \tag{15}$$

where Γ_j is the boundary of the 'j' element.

Eq. (13) can be discretized for a given point 'i' before applying any boundary conditions, as follows

$$\frac{1}{2}\phi^i + \sum_{j=1}^n \int_{\Gamma_j} p\phi d\Gamma = \sum_{j=1}^n \int_{\Gamma_j} wq d\Gamma \quad (i = 1, 2, \dots, n) \quad (16)$$

where

$$\begin{aligned} \phi &= \mathbf{N}^T \phi_j \\ \mathbf{q} &= \mathbf{N}^T \mathbf{q}_j \end{aligned} \quad (17)$$

The point i is one of the boundary nodes. Where ϕ_j and \mathbf{q}_j are the column vectors of ϕ and \mathbf{q} of the 'j' element at node i . Assume that the element node number is n , i.e., $\phi_j = [\phi_1, \dots, \phi_n]^T$ and $\mathbf{q}_j = [q_1, \dots, q_n]^T$. Where \mathbf{N} in Eq. (17) is shape function of the element. When the type of the element is determined, \mathbf{N} is known function.

Secondly, substituting the Eq. (17) into (16) gives

$$\frac{1}{2}\phi^i + \sum_{j=1}^n \int_{\Gamma_j} \mathbf{p}\mathbf{N}^T d\Gamma \phi_j = \sum_{j=1}^n \int_{\Gamma_j} \mathbf{w}\mathbf{N}^T d\Gamma \mathbf{q}_j \quad (18)$$

Using the following notations

$$H_{ij} = \int_{\Gamma_j} \mathbf{p}\mathbf{N}^T d\Gamma + \frac{1}{2}\delta_{ij}, G_{ij} = \int_{\Gamma_j} \mathbf{w}\mathbf{N}^T d\Gamma$$

Finally, the BEM equation is expressed as

$$\sum_{j=1}^n H_{ij} \phi_j = \sum_{j=1}^n G_{ij} q_j \quad (i = 1, 2, \dots, n) \quad (19)$$

These equations can be written in matrix forms as

$$\mathbf{H}\Phi = \mathbf{G}\mathbf{Q} \quad (20)$$

where \mathbf{H} and \mathbf{G} are two $n \times n$ matrices and Φ and \mathbf{Q} are vector of length n , i.e.,

$$\mathbf{H} = \begin{bmatrix} H_{11} & H_{12} & \dots & H_{1n} \\ H_{21} & H_{22} & \dots & H_{2n} \\ \dots & \dots & \dots & \dots \\ H_{n1} & H_{n2} & \dots & H_{nn} \end{bmatrix}, \quad \mathbf{G} = \begin{bmatrix} G_{11} & G_{12} & \dots & G_{1n} \\ G_{21} & G_{22} & \dots & G_{2n} \\ \dots & \dots & \dots & \dots \\ G_{n1} & G_{n2} & \dots & G_{nn} \end{bmatrix}$$

$$\Phi = [\phi_1, \phi_2, \dots, \phi_n]^T, \quad \mathbf{Q} = [q_1, q_2, \dots, q_n]^T$$

Notice that each node, either \mathbf{q} or ϕ is given. In the paper, $\mathbf{q}_j (j = 1, \dots, n)$ on boundary is known, and there are only $\phi_j (j = 1, \dots, n)$ unknown in the set of equations. Solving the Eq. (20), one can obtain values of ϕ 's. Furthermore, both \mathbf{q} and ϕ are known.

The BEM theory above is employed to calculate the potential values of flow field around the membrane structure. Introducing the potential value into Eq. (1), it is easy to get the velocities of the flow around the structure. Then we can compute the distribution of wind pressure combining with Bernoulli equation (Eq. (3)). The procedure of fluid-structure interaction is considered a steady state and static in this research. Accordingly, in the equations mentioned above, all the items are independent of time. Further research on the time-domain boundary element method may be carried out in the future (Carrer and Mansur 2006).

4. Computation of the structural deformation

The membrane structural simulations are performed by the finite element software ANSYS. And triangular shell41 elements are selected in surface meshing. When mesh the elements of structural surface, we adopt the same nodes to the corresponding nodes of 4-noded quadrilateral elements on the boundary of air flow. The data exchange takes place at the coincident nodes between CFD module and CSD module. i.e., in CFD module, we obtain the wind pressure at coincident nodes of 4-noded quadrilateral elements; Then the pressure of which nodes are applied to the same nodes of triangular shell41 elements in CSD module; Afterwards, we could achieve the nodal displacements of triangular shell41 elements; The next step is applied the displacements to the nodes of 4-noded quadrilateral elements in CFD module. As the nodes of fluid and structure coincide on the same surface, the interpolation codes are not necessary any more. Consequently, the computational efficiency is enhanced.

5. Calculation steps of fluid-structure coupling

Based on the theories mentioned above, in uniform flow, the fluid-structure interaction calculation procedure is as follows

(1) For a given membrane structure, BEM is employed to calculate the potential values in the flow field around the initial structural form. Substituting potential into Eq. (1) and Eq. (3), \mathbf{p}_0 is obtained, i.e., the wind pressure distribution on the structural surface.

(2) Software ANSYS is employed to calculate the deformation \mathbf{x}_0 of the membrane structure under wind pressure \mathbf{p}_0 .

(3) According to the deformation \mathbf{x}_0 , modify the shape of membrane structure. Compute the distribution of wind pressure \mathbf{p}_1 on the deformed structure.

(4) The structural deformation \mathbf{x}_1 under wind load \mathbf{p}_1 is performed with ANSYS.

(5) The iterative procedure (step (3) and step (4)) will not stopped until the solution is satisfied the convergence criterion, i.e., $\mathbf{x}_i \approx \mathbf{x}_{i-1}$. At that moment, the system is in a steady state, and \mathbf{p}_i and \mathbf{x}_i denote the distribution of wind pressure on the structural surface and the corresponding structural deformations respectively.

The mean and variance of the displacement differences between two loops are selected as convergence criterion. It means only if the computational results are less than a certain barrier (convergence criterion), the iterative procedure ends.

Fig. 2 shows the flowchart of the coupling procedure mentioned above.

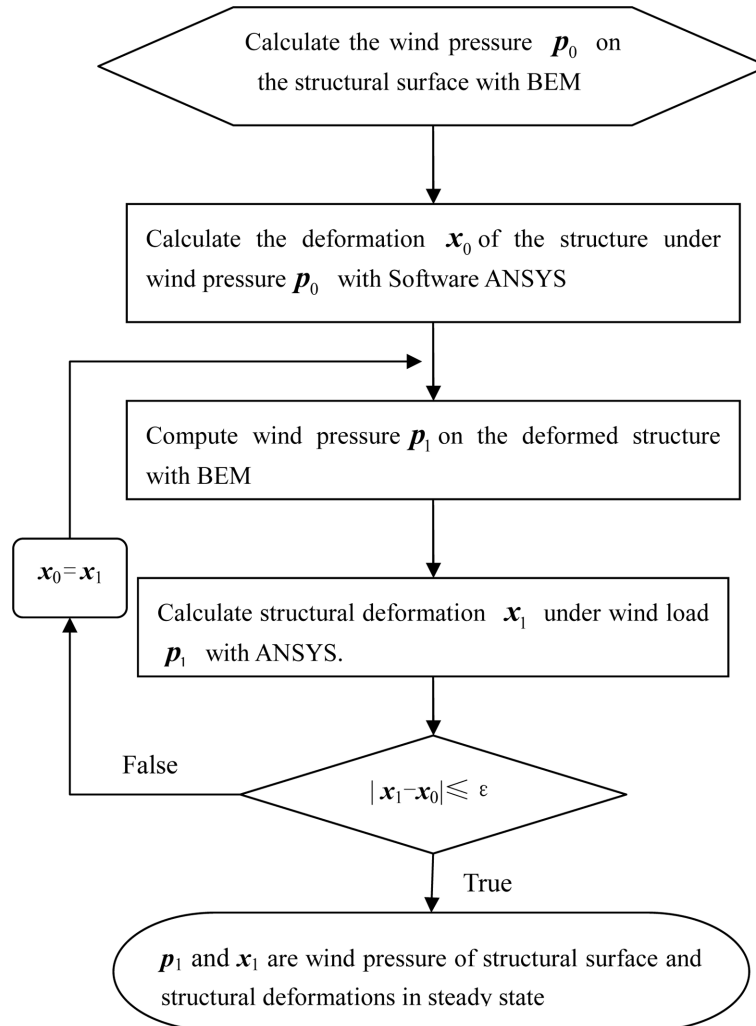


Fig. 2 Flow chart for the strategy of interaction

6. Numerical examples

The coupling procedure presented in the previous sections was applied to several cases, as follows:

Example 1 A two-dimensional closed long span flat roof (see Fig. 3)

The following example presents a closed long span flat roof under wind load. In order to increase computational efficiency, the depth of channel is limited and appropriate fluid boundary conditions applied to reduce the problem to two-dimension. The flexible roof is treated as cable elements. The parameters used in the analysis are assumed $H = 10$ m, $L = 40$ m, $V = 20$ m/s, $g = 5$ kg/m, $Et = 2550$ N/cm, $T = 20$ KN/m, where H is the height of roof, L is span, V is the entrance wind velocity, g is mass per unit length, Et is tensile stiffness and T is pretension.

Linear boundary elements are used to calculate flow field. Considering the influence of the corner nodes on the structure, the elements near those nodes are refined to improve the accuracy of

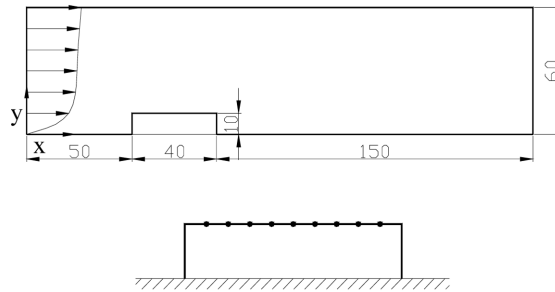


Fig. 3 A two-dimensional closed long span flat roof

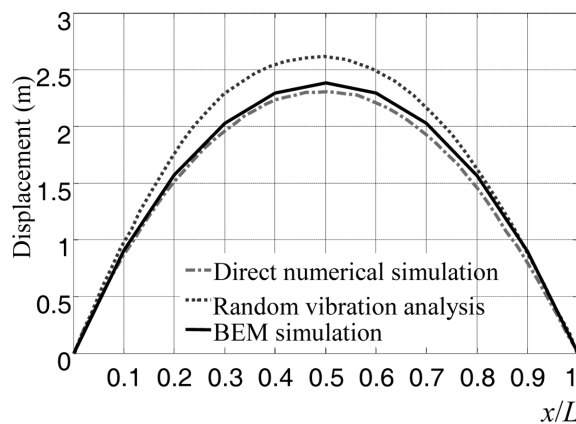


Fig. 4 Max. response of flat roof

solutions. Using software ANSYS, the roof is discretized by link10 in structural simulation. The displacement of the roof in steady state is marked as solid line in Fig. 4. The dot line in the same figure denotes the maximal structural displacements basing on the stochastic vibration time-history analysis method and the dot dash line represents the maximal structural displacements adopting direct numerical simulation method (Sun 2006). As the fluid-structure interaction is considered in BEM method (presented in this study) and the numerical simulation method (in reference Sun 2006), the two displacement curves produced by these two methods are closed. However, the fluid-structure interaction does not take into account in the stochastic vibration time-history analysis method. Hence, the displacements calculated by this method are much greater than those simulated by the other two method mentioned above.

Example 2 Saddle membrane structure (see Fig. 5 and Fig. 6)

In what follows is an example of a closed saddle membrane structure supported by rigid boundary. The direction of incoming flow is 45° and entrance wind velocity is 20 m/s. The parameters induced in this case are assumed $L = 28$ m, $f/L = 1/12$, $T = 2.5$ KN/m, $t = 0.001$ m, $g = 1.25$ kg/m, $Et = 2550$ N/cm, $Gt = 800$ N/cm, $\mu = 0.3$, where L is span, f/L is rise-span ratio, T is initial pretension, t is the thickness of film, g is mass per unit length, Et is tensile stiffness, Gt is shear stiffness and μ is Poisson's ratio. The 4-noded quadrilateral boundary elements are used to calculate flow field. As shown in Fig. 7-Fig. 9, the whole flow field is divided into 5769 units, including 900 units on the coupling surface. And shell41 elements of ANSYS are applied in structural simulation (see Fig. 10).

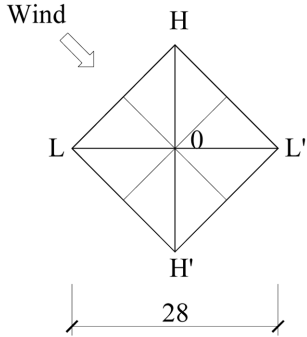


Fig. 5 Sketch of saddle membrane structure top view

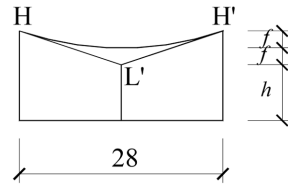


Fig. 6 Sketch of saddle membrane structure side view

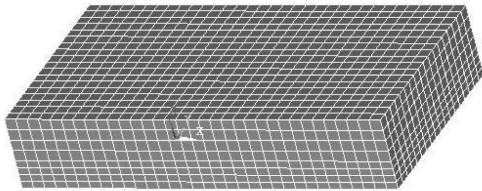


Fig. 7 Flow field: 3D view of mesh

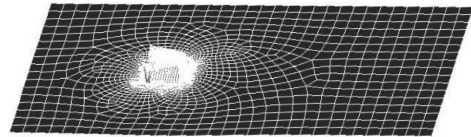


Fig. 8 Flow field: bottom view of mesh

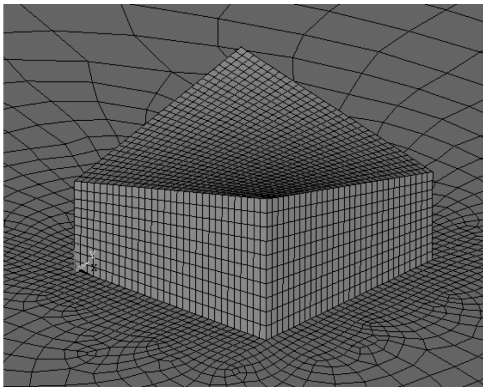


Fig. 9 flow field partial enlarged detail of mesh

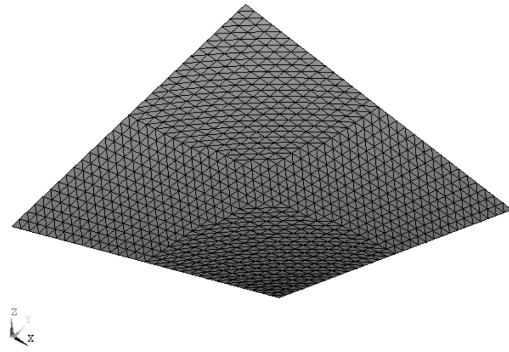


Fig. 10 Structure field: 3D view of mesh

Primarily, the simulation of flow field needs to be validated. Due to lacks of aeroelastic model data, we contrast the wind pressure coefficient distribution to which of wind tunnel rigid model, where the former is achieved in the step (1) in fluid-structure coupling. The wind tunnel test has been carried out in HD-2 wind tunnel of Wind Engineering Reseach Certer of Hunan University. The saddle model is the rigid and made of inorganic glass. The raise-span ratio of this model is 1/12 and the geometry scale is 1/200. At the same time, the Strouhal number is taken into account in the model. Fig. 11 shows the wind pressure distribution of model. The wind pressure coefficient distribution is illustrated in Fig. 12, which is obtained by the method present in this paper.

Comparing with the results of wind tunnel test, the wind pressure coefficient distribution of the numerical example is basically identical and the values of wind pressure coefficient are slightly

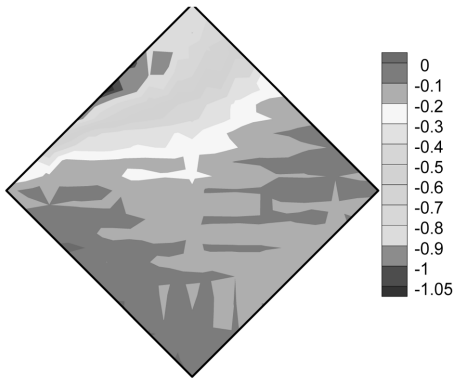


Fig. 11 Wind pressure coefficient distribution of wind tunnel model

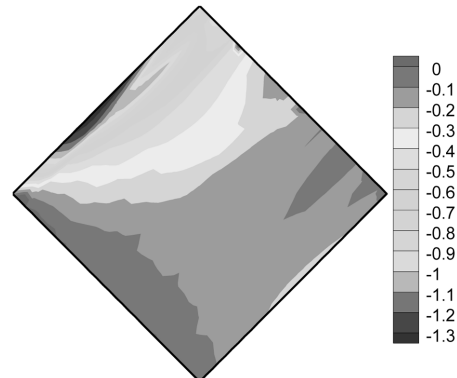


Fig. 12 Wind pressure coefficient distribution of example 2 adopting BEM

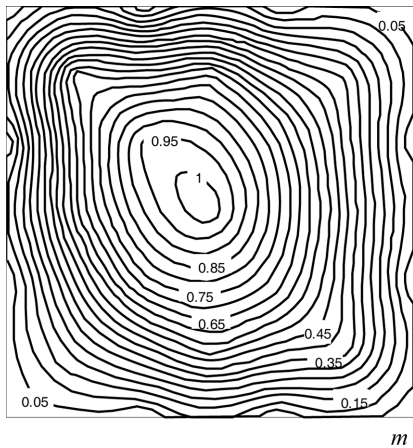


Fig. 13 Maximum displacement of the membrane structure adopting direct numerical simulation method

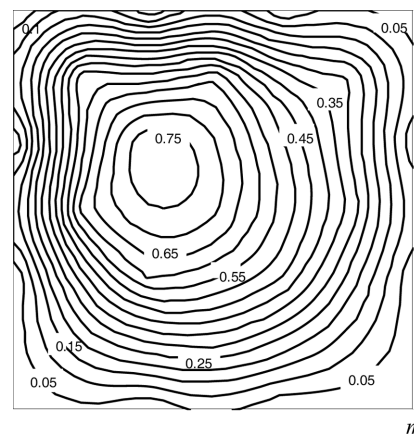


Fig. 14 Maximum displacement of the membrane structure adopting random vibration time-history analysis method

difference (see Fig. 11 and Fig. 12). Particularly, in the major part region of structure surface, the wind pressure coefficient distribution is similar. However certain differences exist in edge region. Adopt the potential flow hypothesis and neglect the vortex effect caused by viscosity of air, which is one of main reason for the differences. Another main reason is that the acute angles (i.e., structure edges) of the non-smooth regions in the flow field will produce error by using boundary element method. Fortunately, the influence scope of error is restricted within narrow limits around acute angles. Hence, the wind pressure distribution simulated by using boundary element method is acceptable.

The validity of example 2 has been tested in contrast with the example in reference (Sun 2006). The maximum structural displacements are shown in Fig. 13, which was calculated in the direct numerical simulation method and considered the influence of fluid-structure interaction. While Fig. 14 shows the maximum structural displacements based on the random vibration time-history analysis method and omitted the wind-structure coupling. The results in steady state obtained from

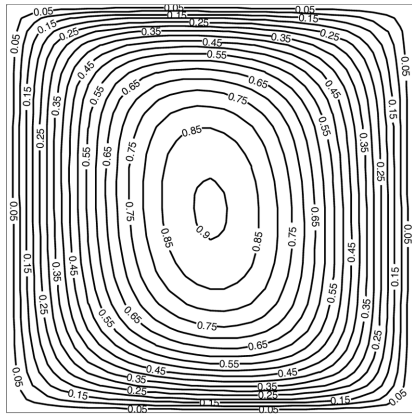


Fig. 15 $V = 20$ m/s, $f = 1/12$, $T = 2.5$ KN/m Maximum displacement of the membrane structure adopting BEM

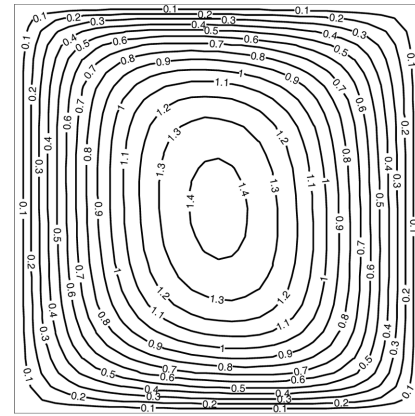


Fig. 16 $V = 25$ m/s Maximum displacement of the membrane structure adopting BEM

the method provided in this paper are presented in Fig. 15. It is observed that the values in Fig. 15 are a little lower than those in Fig. 13. In other words, the displacements simulated in BEM are less than those based on the direct numerical simulation method. The reason is that the flow in present study is uniform potential and the effect of fluctuating flow is omitted. The distributions of displacements in Fig. 15 are consistent with those in Fig. 13 mostly. However, certain differences of displacements exist in edges of the membrane. Similarly, the main reasons for the differences of displacements are potential flow hypothesis and acute angles of the non-smooth regions mentioned above. These two examples cited above have validated the feasibility of the algorithm presented in this paper.

Considering the reasons for differences of wind pressure distribution on edges, the application range of the method presented in this paper is restricted within the following: the membrane structure is the enclosed construction. There are no projecting parts on the membrane surface, such as cornices and so on. The flow in the fluid field is the potential. Thereby turbulence in air is not taken into account.

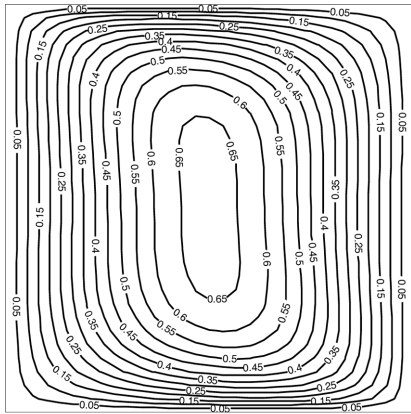
In what follows the various parameters of the membrane structures and flow field will be investigated in process of wind-structure interaction.

Example 3: Change the structural rise-span ratio, i.e., $f/L = 1/6$, and other conditions are same to example 2.

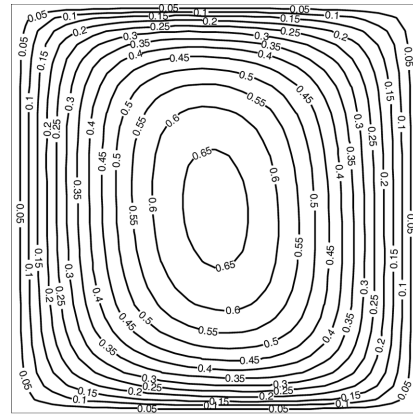
Example 4: Change structural initial pretension, i.e., $T = 4.0$ KN/m, and other conditions are same to example 2.

Example 5: Change the entrance velocity, i.e., $V = 25$ m/s, and other conditions are same to example 2.

Contrasting Fig. 15 and Fig. 16, when the speed of the entrance wind velocity is higher, the deformations of membrane structures increase correspondingly, nevertheless the distribution of these two figures are similar. With the raising of structural rise-span ratio, the geometric stiffness is strengthened. Consequently, the structural capacity to resist deformation is enhanced, thus, the displacements are reduced (see Fig. 15 and Fig. 17). The structural shape and distribution of wind pressure change with different rise-span ratio. As a result, deformations of structures, whose rise-



m



m

Fig. 17 $f=1/6$ Maximum displacement of the membrane structure adopting BEM

Fig. 18 $T=4.0$ KN/m Maximum displacement of the membrane structure adopting BEM

span ratios are different, are not coincident, especially in the mid surface. Comparing Fig. 18 with Fig. 15, the deformations decrease with the increase of initial pretension force but the trend of deformation does not change in the same flow field conditions. The reason is that the increase of initial pretension force strengthen stiffness of structure, however, the structural shape maintains the original profile.

In computation process, convergence criterion is the mean and variance of the displacement differences between two loops. Such as the examples of membrane structures mentioned in previous parts, when the mean and variance of displacement differences are less than 0.02 m and 0.0003 m², the iterative procedure ends. Generally speaking, the loops will be executed six to eight times before the convergence criterion is satisfied, and one loop of the iterative procedure will cost 2 hours to 3 hours. Comparing with the series of software CFD, BEM saves a great amount of consuming time in the flow field. However, BEM is limited to solve problems in potential flow field, i.e. several factors can not be considered in the flow field in BEM, such as turbulence models, boundary layer and so on. Comparing with BEM, the flow field simulated by CFD software is more close to reality. Even so, structural displacements distribution calculated by BEM at steady state is closed to those based on CFD numerical simulation (see reference Sun 2006), which implies the method presented in this paper is acceptable.

7. Conclusions

An efficient numerical method based on BEM has been described, which can deal with wind-structure interaction at steady state in uniform flow. Simple accurate methods just like the one suggested in the paper are essential in order to contain computational costs for the practical membrane structures. The computation time of BEM is less than that in CFD numerical simulation. One reason is that the elements are discretized just on the boundary of flow field in this method, but in CFD software the whole domain should be meshed. Especially in large 3D problems, the superiority in meshing time is remarkable. Another reason is that the nodes of fluid based on BEM

elements and those of structure solved with software ANSYS elements are coincide on wetted surface, and the interpolation codes are not necessary any more in this situation. Comparing with the cases based on CFD numerical simulation, this method has been examined and proved effective and reliable. However, this method is not suitable for the structures with projecting parts on the surface.

Numerical cases indicate that deformations of the saddle membrane structures increase, taking into account of the effect of wind-structure interaction, in 45 degree incoming flow. Furthermore, the deformations increase with enhance of entrance wind velocity. But the distribution rules of displacements do not change with that generally. While raise structural rise-span ratio or increase initial pretension force, the stiffness of structure is strengthened, which causes the structural deformations to reduce.

Acknowledgements

Financial support by the National Natural Science Foundation of China is gratefully acknowledged. The authors also want to thank Dr. Gao xiao-wei for technical support as well as some worthwhile discussions.

References

- Brebbia, C.A. and Dominguez, J. (1992), *Boundary Elements an Introductory Course*, 2nd ed., Computational Mechanics Publications & McGraw-Hill, NY.
- Carrer, J.A.M. and Mansur, W.J. (2006), "Solution of the two-dimensional scalar wave equation by the time-domain boundary element method: Lagrange truncation strategy in time integration", *Struct. Eng. Mech.*, **23**(3), 263-278.
- Forster, B. and Mollaert, M. (2004), *European Design Guide for Tensile Surface Structures*, TensiNet, Brussels
- Gao, X.W. and Davies, T.G. (2002), *Boundary Element Programming in Mechanics*, Cambridge University Press, Cambridge, UK; NY.
- Giovanni, S. (2002), "The role of analytical methods for evaluating the wind-induced response of structures", *J. Wind Eng.*, **90**(12-15), 1453-1477.
- Glück, M., Breuer, M., Durst, F., Halfmann, A. and Rank, E. (2003), "Computation of wind-induced vibrations of flexible shells and membranous structures", *J. Fluid. Struct.*, **17**(5), 739-765.
- Glück, M., Breuer, M., Durst, F., Halfmann, A. and Rank, E. (2001), "Computation of fluid-structure interaction on lightweight structures", *J. Wind Eng.*, **89**(14-15), 1351-1368.
- Hübner, B., Walborn, E. and Dinkler, D. (2002), "Simultaneous solution to the interaction of wind flow and lightweight membrane structures", *Proceedings of International Conference on Lightweight Structures in Civil Engineering*, Warsaw.
- Irwin, H.P.A.H. and Wardlaw, R.L. (1979), "A wind tunnel investigation of a retractable fabric roof for the Montreal Olympic stadium", *Proceedings of 5th International Conference on Wind Engineering*, Colorado.
- Minami, H. (1998), "Added mass of a membrane vibrating at finite amplitude", *J. Fluid Struct.*, **12**(7), 919-932.
- Pospisil, S., Naprstek, J. and Hracov, S. (2006), "Stability domains in flow-structure interaction and influence of random noises", *J. Wind Eng.*, **94**(11), 883-893.
- Shen, S.Z. and Wu, Y. (2006), "Research progress on fluid-solid interaction effect of wind-induced vibration response of membrane structure", *J. ARCH. CIV. E.*, **23**(1), 1-9.
- Sun, B.N., Mao, G.D. and Lou, W.J. (2003), "Wind-induced coupling dynamic response of closed membrane structure", *Proceedings of 11th International Conference on Wind Engineering*, Texas, June.
- Sun, X.Y. (2006) "Study on Wind-Structure Interaction in Wind-induced Vibration of Membrane Structures",

- Ph.D. thesis. Harbin Institute of Technology.
- Sygulski, R. (1997), "Numerical analysis of membrane stability in air flow", *J. Sound Vib.*, **207**(3), 281-292.
- Theodore, S. (1997) "Computational wind engineering: Past achievements and future challenges", *J. Wind Eng.*, **67&68**, 509-532.
- Uematsu, Y. and Uchiyama, K. (1986), "Aeroelastic behavior of an H.P.-shaped suspended Roof, Shells, Membranes and Space Frames", *Proceedings IASS Symposium*, Osaka.
- Wüchner, R., Kupzok, A. and Bletzinger, K.U. (2007), "A framework for stabilized partitioned analysis of thin membrane-wind interaction", *Int. J. Numer. F.*, **54**(6-8), 945-963.
- Yadykin, Y., Teneto, V. and Levin, D. (2003), "The added mass of a flexible plate oscillating in a fluid", *J. Fluid Struct.*, **17**(1), 115-123.
- Zhang, L.Q., Wu, Y. and Shen, S.Z. (2002), "Aerodynamic damping identification of cable-membrane structures under wind-induced vibration", *Proceedings of 11th National Conference on Structural Wind Engineering*, Sanya.

Appendix

$$\delta_{ij} = 1 \text{ when } i = j$$

$$\delta_{ij} = 0 \text{ when } i \neq j$$

Dirac delta function $\delta(x, p)$

$$\int_{-\infty}^{\infty} \delta(x, p) dx = \int_{p+\varepsilon}^{p-\varepsilon} \delta(x, p) dx = 1$$

where p is the singular point and ε denotes a vanishingly small radius of integration around this singularity.

$$\int_{-\infty}^{\infty} f(x) \delta(x, p) dx = \int_{p+\varepsilon}^{p-\varepsilon} f(x) \delta(x, p) dx = f(p)$$